ELSEVIER

Earth and Planetary Science Letters 144 (1996) 529–546

EPSL

Os, Sr, Nd, Pb, O isotope and trace element data from the Ferrar flood basalts, Antarctica: evidence for an enriched subcontinental lithospheric source

M. Molzahn [a,b], L. Reisberg [c], G. Wörner [b,d,*]

[a] *Max Planck Institut für Chemie, Postfach 3060, 55020 Mainz, Germany*
[b] *Institut für Geowissenschaften, Universität Mainz, 55099 Mainz, Germany*
[c] *CNRS / CRPG, BP 20, 54501 Vandœuvre-les-Nancy, France*
[d] *Geochemisches Institut, Universität Göttingen, Goldschmidtstrasse 1, D-37077 Göttingen, Germany*

Received 29 January 1996; revised 9 September 1996; accepted 12 September 1996

Abstract

Os, Sr, Nd, Pb and O isotopes and trace element data are reported for basaltic andesite and andesite whole rocks and, in part, for selected mineral separates from the Jurassic Ferrar flood basalt province. Radiogenic Sr (> 0.709), unradiogenic Nd ($\epsilon_{Nd} = -3$ to -5), and radiogenic Pb isotopes, as well as low Nb/La ratios of 0.4–0.6 and Nb/La ratios between 0.45 and 0.6 are found for all rocks including our most primitive sample (Mg# = 71.9). This indicates involvement of either continental crust or enriched lithospheric mantle in magma genesis. $^{187}Re/^{188}Os$ correlates strongly with $^{187}Os/^{188}Os$, with an age of 172 ± 5 Ma, in agreement with published Ar–Ar data. Initial $^{187}Os/^{188}Os$ of 0.194 ± 0.023 is close to the range of typical mantle values for MORB, OIB and lithospheric mantle and much lower than that of continental crust. $\delta^{18}O$ values between 5‰ and 7‰ were obtained on fresh bulk samples, separated plagioclases and clinopyroxenes. Sr–O and Sr–Os isotope mixing calculations between depleted mantle peridotite or mantle melts and crustal material rule out assimilation involving basalts with low Os concentrations, and simple binary mixing or pure AFC processes involving picrites. AFC processes, combined with continuous replenishment of picritic magmas, can explain the isotopic data, provided the crustal end-member has high $^{87}Sr/^{86}Sr$ and low $\delta^{18}O$ values. However, lower crustal samples displaying these characteristics are absent in the Ferrar region, and are also unlikely to impart the sediment-like trace element patterns observed in the Ferrar data. A more likely explanation is a lithospheric source enriched by subducted sediments. A contribution to Ferrar magmatism from a plume cannot be distinguished.

Keywords: Ferrar Group; flood basalts; magma contamination; geochemistry

1. Introduction

Continental flood basalts represent large igneous provinces (LIPs, [1–4]) produced over relatively short times. Their origin remains a subject of controversy.

* Corresponding author. Fax: +49 551 393982. E-mail: gwoerne@gwdg.de

PII S0012-821X(96)00178-1

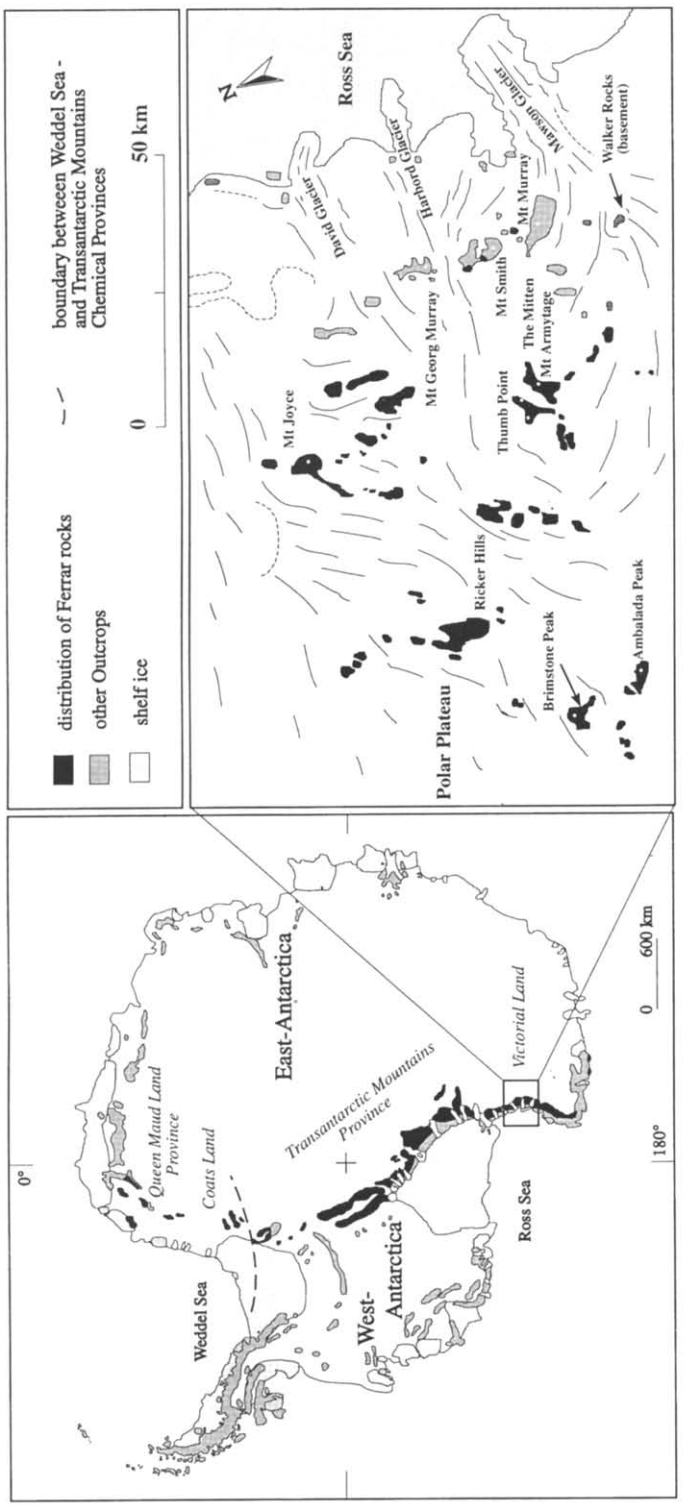

Fig. 1. Map of the study area in the Prince Albert Mountains, Victoria Land, Antarctica.

According to one interpretation, LIPs are induced by the arrival of a new plume head below continental lithosphere. Other authors believe flood basalts result from lithospheric rifting and subsequent upwelling and extensive melting of anomalously hot mantle [1–4]. Plume and asthenospheric material provide major sources for flood basalt provinces. However, heating by the plume and rising magmas may cause additional melting of lithosphere. As a result, many flood basalts have enriched geochemical and isotopic signatures, but it has been difficult to distinguish between magma sources in the crustal and enriched mantle lithosphere. Jurassic Ferrar flood basalts provide an excellent opportunity to examine this problem. These basalts exhibit evidence of lithospheric involvement, including strong enrichment of large ion lithophile elements and Pb, enrichment of in rare earth elements, negative (Ta)–Nb anomalies, radiogenic Sr and Pb isotopes, and unradiogenic Nd isotopes (Table 1). These systematics are observed even for very mafic rocks. Still stronger 'crustal' signatures have been documented for evolved rocks [5–7]. These unusual characteristics have been explained by extensive (lower) crustal contamination of a depleted mantle-derived magma [5–8], or melting of an enriched subcontinental mantle lithosphere [9–12].

We have measured Os isotope compositions in a suite of whole rock samples from Ferrar flood basalts (Victoria Land, Antarctica) along with Sr, Nd, Pb, and O isotopes and trace elements in order to address this controversy. The Re–Os system is useful because ^{187}Re is slightly incompatible during mantle melting, while the daughter ^{187}Os is highly compatible and remains in the residue. This contrasting geochemical behaviour results in low $^{187}Os/^{188}Os$ ratios for primitive mantle material ($^{187}Os/^{188}Os \approx 0.120–0.130$) and a much higher $^{187}Os/^{188}Os$ ratio for average crust (> 1.2) [13–18]. Re–Os isotope analyses of continental flood basalts are still rare [19,20] but include analyses of picrites from the Karoo flood basalt province of southern Africa [19]. In that case, Os isotopes were successfully used to define the source as a mixture of enriched subcontinental lithosphere and plume-derived mantle.

We argue that our data largely rule out crustal assimilation and support the model of an old, enriched, subcontinental mantle lithospheric source for the Ferrar province. Our results also define a Re–Os isochron with an age that agrees with the emplacement age determined from Ar–Ar measurements [21].

2. Setting

Ferrar flows and sills crop out over 3500 km along the Transantarctic Mountains (TAM), which divide the Antarctic continent into an eastern and western part. The province crosses several crustal domains, from the accreted Gondwana margin in Northern Victoria Land towards the East Antarctic Craton in the Queen Maud Land province (Fig. 1). Ferrar magmatism has been related to continental rifting and the break-up of Gondwana in the Jurassic [9,22,23].

Our samples were collected during the GANOVEX VI and VII Expeditions in Northern Victoria Land. The basement in this region comprises three terranes, from west to east: the Wilson Terrane, the Bowers Terrane and the Robertson Bay Terrane, which were juxtaposed during the Ross Orogeny (520–460 Ma; [24–26]). The Wilson Terrane represents the Precambrian western Gondwana margin overprinted by later terrane collisions. The Bowers Terrane is formed by a sequence of metamorphic clastic sediments and volcanics, representing an accreted island arc. Metamorphosed turbidites characterize the Robertson Bay Terrane. Crust and the mantle lithosphere underlying the Ferrar province are thus Precambrian in age. More specifically, the basement, as exposed at Walker Rocks some 50–100 km from our sampling sites, consists of Precambrian shales intruded by the I- to S-type granite Harbour Intrusives (550–500 Ma) and the Admiralty Intrusives (ca. 400 Ma, I-type). In the Devonian to Triassic, clastic sediments of the Beacon Supergroup [26] were deposited unconformably on the basement rocks. Tertiary rifting resulted in the Ross Sea embayment and associated alkaline volcanic rocks.

Sills from the Ferrar Supergroup intrude flat-lying sediments and, rarely, the metamorphic basement. Ferrar lavas cap the sequence, building a flood basalt sequence 700–800 m in height. Recent Ar–Ar dating indicates an emplacement age for sills and flows of about 177 ± 0.2 Ma [21]. A younger thermal alter-

Table 1
Isotope and trace element data of Ferrar whole rock samples from the Prince Albert Mountains, Victoria Land, Antarctica

Sample:	BRI-03	BRI-29	MUR-04	MJY-01	MJY-02	RIH-02	TPS-02
Location:	Brimstone Peak	Brimstone Peak	Mount Murray	Mount Joyce	Mount Joyce	Ricker Hills	Thumb Point
Type:	low-Ti flow	high-Ti flow	low-Ti sill	low-Ti sill	low-Ti sill	low-Ti sill	low-Ti sill
Sample type:	whole rock	whole rock	whole rock	whole rock	whole rock	whole rock	whole rock
Re (ppt)	457	828	336	484	391	433	215
	498	822	324			417	274
							174 [d]
Os [ppt]	7.51	3.98	6.33	7.93	9.74	4.39	18.1
	7.09		7.56				15.2 [d]
$^{187}Re/^{188}Os$	322	**1598**	**277**	**316**	**203**	**581**	59
	343		231				**71** [d]
$^{187}Os/^{188}Os$ [a]	1.070 ± 0.012	**4.892 ± 0.044**	**0.950 ± 0.006**	**0.883 ± 0.004**	**0.692 ± 0.008**	**2.022 ± 0.019**	0.463 ± 0.014
	1.108 ± 0.012		0.934 ± 0.009				**0.475 ± 0.004** [d]
$^{187}Os/^{188}Os$ [b]	0.134 ± 0.073	0.248 ± 0.172	0.145 ± 0.076	[c]	0.102 ± 0.054	0.334 ± 0.114	0.293 ± 0.040
	0.113 ± 0.076		0.261 ± 0.069				0.270 ± 0.020 [d]
Rb (ppm)	19.7	64.0	24.0	40.1	30.2	49.3	21.1
Sr (ppm)	138.1	128.2	125.2	136.8	128.1	136.7	106.6
	135.7	127.6					
$^{87}Rb/^{86}Sr$	0.413	1.444	0.556	0.849	0.681	1.043	0.573
	0.420	1.451					
$^{87}Sr/^{86}Sr$ [a]	0.71122 ± 2	0.71323 ± 1	0.71278 ± 2	0.71377 ± 1	0.71339 ± 2	0.71469 ± 1	0.71316 ± 1
	0.71122 ± 1	0.71320 ± 2					
$^{87}Sr/^{86}Sr$ [b]	0.71017	0.70958	0.71137	0.71162	0.71166	0.71205	0.71171
	0.71016	0.70953					
Sm (ppm)	27.0	6.9	3.0	3.7	3.0	4.6	2.1
Nd (ppm)	11.3	28.4	10.3	15.9	12.5	19.9	7.7
$^{147}Sm/^{144}Nd$	0.145	0.146	0.172	0.140	0.142	0.139	0.164
$^{143}Nd/^{144}Nd$ [a]	0.51241 ± 1	0.51240 ± 2	0.51231 ± 1	0.51231 ± 1	0.51231 ± 1	0.51230 ± 1	0.51231 ± 2
$^{143}Nd/^{144}Nd$ [b]	0.51224	0.51223	0.51211	0.51215	0.51215	0.51214	0.51212
ϵNd [b]	−3.2	−3.5	−5.8	−5.0	−5.1	−5.2	−5.6
$\delta^{18}O$	8.03	6.01	6.52	7.01	6.27	4.79	6.29
V	215	422	228	236	241	237	192
Cr	135	8	133	94	116	41	296
Co	39	47	44	42	42	42	53
Ni	73	23	79	71	83	48	167
Cu	79	219	58	80	67	99	58
Zn	74	133	69	84	75	97	71
Y	19	45	16	22	19	27	14
Zr	107	430	97	143	119	198	54
Nb	4.9	13.1	4.4	6.9	5.2	10.7	3.7
Ba	180	372	132	212	172	325	160
Ga	14.2	20	14.8	15.8	15.6	16.8	13
Pb	4.6	11.2	4.3	6.6	5.2	9.4	3.4
Th	4	7.4	3.5	5.2	3.5	10.1	3.6
U	0.9	2	0.5	1	0.8	1.9	0.5
Li	10.3	26.5	9	11.2	13.8	21.6	7.9
Sc	50	52	53	49	54	42	52
Cs	0.4	1.8	1.3	2.3	1	1.5	0.8
Hf	3	7.2	2.7	4	3.3	3.5	1.6
Ta	0.57	0.96	0.84	1.03	0.51	0.87	0.57
La	10.2	25.4	9.1	13.8	11.2	20.3	6.6
Ce	22	51	18	28	22	42	14
Pr	3	7.5	2.7	4.1	3.3	5.6	1.9
Eu	0.8	1.9	0.8	1.1	1	1.2	0.5

Table 1 (continued)

Sample:	BRI-03	BRI-29	MUR-04	MJY-01	MJY-02	RIH-02	TPS-02
Location:	Brimstone Peak	Brimstone Peak	Mount Murray	Mount Joyce	Mount Joyce	Ricker Hills	Thumb Point
Type:	low-Ti flow	high-Ti flow	low-Ti sill	low-Ti sill	low-Ti sill	low-Ti sill	low-Ti sill
Sample type:	whole rock	whole rock	whole rock	whole rock	whole rock	whole rock	whole rock
Gd	3.2	7.7	2.8	4.2	3.5	4.1	2.2
Tb	0.53	1.28	0.46	0.66	0.56	0.82	0.34
Dy	3.3	8	3	4.2	3.5	4.5	2.4
Ho	0.71	1.71	0.62	0.87	0.76	0.94	0.5
Er	2.2	5	1.9	2.7	2.3	2.8	1.6
Tm	0.32	0.73	0.28	0.39	0.33	0.43	0.21
Yb	2.2	5.2	1.9	2.7	2.3	2.7	1.6
Lu	0.32	0.73	0.29	0.40	0.35	0.44	0.23

Re and Os concentrations (ppt) by isotope dilution. $^{187}Os/^{186}Os$ ratio calculated from $^{187}Os/^{188}Os$ using the natural $^{187}Os/^{188}Os$ ratio (0.12035). Methods were similar to those described in [15], except that Re and Os were determined on separate powder splits. Both elements were measured on Pt filaments using the Finnigan MAT262 mass spectrometer of CRPG/CNRS (Nancy, France). Total procedural blanks varied from 1 to 2 pg for Os and from 9 to 50 pg for Re.

[a] Present isotopic ratio. [b] Initial ratio corrected for an age of 177 Ma. Errors listed for present ratios are 2s-m inrun precisions. Errors for initial $^{187}Os/^{188}Os$ include uncertainties on both analytical precisions and Re and Os blank corrections. Data listed on alternate lines represent repeat analyses of separate powder splits. [c] Age correction resulted in negative value, Fig. 5 plots a value of zero. [d] Data obtained at LDEO.

Re concentrations from the highest quality runs are listed in the first row and used to calculate all corresponding $^{187}Re/^{188}Os$ ratios. The typical error on the $^{187}Re/^{188}Os$ ratio is about ±25 and includes uncertainties on the Re determination and Re blank corrections. Os concentration includes radiogenic ^{187}Os. Data points used for the isochron calculation are given in bold. Sr and Nd isotopes were corrected for fractionation using $^{86}Sr/^{88}Sr = 0.1194$ and $^{146}Nd/^{144}Nd = 0.7129$, respectively. ϵNd values were calculated using $^{143}Nd/^{146}Nd_{CHUR\ today} = 0.512638$ and $^{147}Sm/^{144}Nd_{CHUR\ today} = 0.1966$.

ation of the Ferrar province occurred at c. 100 Ma ([27], and own unpublished data). The bulk of the Ferrar province is basaltic andesite to andesite in composition, basalts are rare. Nevertheless, in accordance with the general custom, we use the term Ferrar 'basalts'.

Ferrar rocks typically have high initial $^{87}Sr/^{86}Sr$ ratios (> 0.708), initial ϵNd values below −3, and radiogenenic Pb isotopes suggesting a lithospheric (crust or mantle) input (Tables 1 and 2; and [5–11]). In contrast, flood basalts of the same age from the Queen Maud Land province in Antarctica (Fig. 1) have lower $^{87}Sr/^{86}Sr$ ratios (< 0.707) and higher initial ϵNd values and were related to a plume [11] and the Karoo flood basalts [28]. Basalts from the intermediate Coats Land region [11] display chemical and isotopic compositions transitional between the two provinces. The Ferrar province was related to an extensional regime of a back-arc environment inboard from the Jurassic Western Gondwana active margin [22]. A plume origin (thermal or chemical) for the Ferrar basalt source is still debated.

3. Methods

Sr, Nd, Pb isotopes were determined at the Max Planck Institute (Mainz) and O isotopes and trace elements by ICP–MS (Göttingen), by standard techniques. Re and Os isotope compositions were measured at the CRPG/CNRS in Nancy following [17]. About 6 g of powder spiked with ^{190}Os were dissolved for 12 h at 110°C in a reducing HCl + HF + ethanol solution, dried down, and taken up in HCl + HF + ethanol five times. Samples were then heated to 140°C in concentrated H_2SO_4. Os was distilled in a two-stage silica glass still from a solution of Cr^{VI} in 5 N H_2SO_4. Oxidized Os was evaporated and transported to 1% H_2O_2 solution in the first step. In the second step, Os from this solution was again vaporized and caught in 9 N HBr. A single bead of CHELEX 20 was used to purify the Os fraction. For Re, about 1.5 g of sample spiked with ^{185}Re was dissolved in a HF:HNO_3 mix at 110°C for 4 days. The Re fraction was separated by loading in 0.8 N HNO_3 onto a cation exchange column (AG 1 × 8

Table 2
Isotope data of separated minerals

Sample name:	BRI-03	BRI-03 (2)	BRI-29	MUR-04	MUR-04 (2)	MJY-01					
	Plag	Cpx	Plag [c]	Cpx	Plag	Cpx	Plag [c]	Cpx	Plag	Cpx	Plag	Cpx
Rb (ppm)	5.1	0.4	15.6	–	16.0	3.2	36.2	0.1	–	–	123.0	0.7
Sr (ppm)	44.0	23.0	38.2	–	323.6	13.1	207.3	6.7	–	–	71.1	15.2
$^{87}Rb/^{86}Sr$	0.33554	0.45756	1.18527	–	0.14288	0.69911	0.50501	0.02576	–	–	5.00752	0.12565
$^{87}Sr/^{86}Sr$ [a]	0.71075	0.71076	0.71071	0.71076	0.71024	0.71132	0.71236	0.71138	–	–	0.72478	0.71179
2σ	2	2	2	2	2	3	2	4	–	–	9	3
$^{87}Sr/^{86}Sr$ [b]	0.70990	0.70960	0.70771	–	0.70988	0.70955	0.71135	0.71131	–	–	0.71211	0.71147
Sm (ppm)	0.03	0.5	–	–	0.7	6.5	0.6	1.3	1.4	–	0.8	2.1
Nd (ppm)	0.1	1.2	0.1	–	29.0	18.7	4.3	3.5	6.3	–	3.5	5.7
$^{147}Sm/^{144}Nd$	0.14469	0.24824		–	0.13651	0.20876	0.08820	0.21693	0.13333	–	0.13078	0.21884
$^{143}Nd/^{144}Nd$ [a]	0.51242	0.51246	0.51246	–	0.51235	0.51244	0.51232	0.51239	0.51227	–	0.51231	0.512244
2σ	4	1	5	–	1	1	2	3	1	–	1	1
$^{143}Nd/^{144}Nd$ [b]	0.51225	0.51217	–	–	0.51219	0.51220	0.51222	0.51214	0.51212	–	0.51216	0.51218
ϵNd [b]	−3.0	−4.5	–	–	−4.3	−4.1	−3.7	−5.2	−5.6	–	−4.8	−4.4
$^{206}Pb/^{204}Pb$	18.55	–	–	–	18.60	–	18.69	–	–	–	18.64	–
$^{207}Pb/^{204}Pb$	15.66	–	–	–	15.58	–	15.63	–	–	–	15.58	–
$^{208}Pb/^{204}Pb$	38.35	–	–	–	38.22	–	38.48	–	–	–	38.27	–
$\delta^{18}O$	13.33	6.18	18.27	–	6.03	5.16	7.77	5.74	–	–	–	–

	MJY-02		RIH-02		TPS-02	
	Plag	Cpx	Plag	Cpx	Plag	Cpx
Rb (ppm)	4.7	1.6	18.2	0.5	0.8	
Sr (ppm)	191.8	7.5	100.7	10.1	66.2	
$^{87}Rb/^{86}Sr$	0.07140	0.63109	0.52180	0.15549	0.03627	
$^{87}Sr/^{86}Sr$ [a]	0.71379	0.71167	0.71416	0.71241	0.71227	
2σ	2	3	2	2	2	
$^{87}Sr/^{86}Sr$ [b]	0.71361	0.71007	0.71284	0.71201	0.71217	
Sm (ppm)	0.7	1.9	0.3	1.6	–	0.3
Nd (ppm)	3.4	5.2	1.1	4.2	0.2	0.9
$^{147}Sm/^{144}Nd$	0.12694	0.22091	0.15203	0.22799	–	0.22731
$^{143}Nd/^{144}Nd$ [a]	0.51231	0.51244	0.51230	0.51244	0.51231	0.51243
2σ	1	2	2	1	2	2
$^{143}Nd/^{144}Nd$ [b]	0.51216	0.51218	0.51212	0.51217	–	0.51217
ϵNd [b]	−4.8	−4.3	−5.5	−4.6	–	−4.7
$^{206}Pb/^{204}Pb$	18.71	–	–	–	18.70	–
$^{207}Pb/^{204}Pb$	15.63	–	–	–	15.65	–
$^{208}Pb/^{204}Pb$	38.44	–	–	–	38.55	–
$\delta^{18}O$	–	–	–	–	6.39	5.84

[a] Present isotopic ratio.

[b] Initial ratio corrected for an age of 177 Ma.

[c] Altered plagioclase, not included in Fig. 5. Age correction using an age of 177 Ma. Pb isotopes not age corrected, assuming that plagioclase is essentially U-free. Sr and Nd isotopes were corrected for fractionation using $^{86}Sr/^{88}Sr = 0.1194$ and $^{146}Nd/^{144}Nd = 0.7129$, respectively. ϵNd values were calculated using $^{143}Nd/^{146}Nd_{CHUR\ today} = 0.512638$ and $^{147}Sm/^{144}Nd_{CHUR\ today} = 0.1966$.

resin) and eluted with 8 N HNO_3. A single bead of AG 1×4 was used to purify the Re fraction. Total blanks were less than 1 pg Os per 1 g of sample and quite variable for Re (about 15 pg per 1 g of sample). Re values presented in Table 1 have been blank corrected.

Os and Re isotope compositions were measured on a Finnigan MAT 262 at the CRPG/CNRS in negative thermal ionization mode [30,31]. Corrections for $^{187}ReO_3$ were made to mass 235 using the mass 233 intensity, on the assumption that this peak consisted solely of $^{185}ReO_3$. This assumption is justified, because changes in the 235/236 ratio during a run correlated with changes in 233/236 intensity.

In order to account for possible problems related to the 'nugget effect' of high Re and Os concentrations in sulphides, we analyzed three samples for Re, Os and Os isotopes and two additional samples for Re twice. Our results (Table 1) show good reproducibility, thus the nugget effect should be minimal. A data set including ICP–MS trace elements can be obtained from the authors on request.

4. Assimilation or a lithospheric mantle source for Ferrar magmatism? Trace element patterns

Spider diagrams (Fig. 2) for Ferrar Lavas have rather low abundance of incompatible elements, between 10 times and 100 times those of primitive mantle [32], with Nd concentrations close to those of

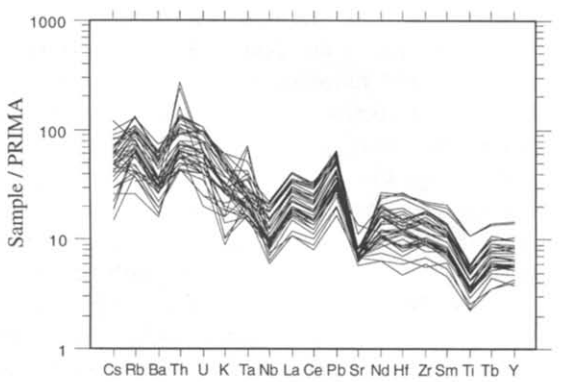

Fig. 2. Multi-element spider diagrams normalized to primitive mantle [32] for Ferrar lavas from Victoria Land.

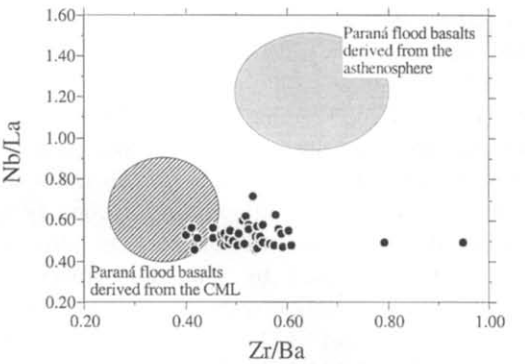

Fig. 3. Nb/La vs. Zr/Ba for Ferrar lavas from Victoria Land. Fields taken from [33].

MORB [10]. The patterns show spikes of enrichment for Th and Pb and depletion for P (not in Fig. 2) and Ti on a slightly incompatible-enriched pattern. Ore and apatite fractionation during differentiation can only partly account for this observation, since even the most mafic sample shows significant P and Ti depletion. Distinct negative spikes also exist for Nb.

Subcontinental lithospheric magma sources for the Paraná province have been shown to be distinct from asthenospheric and/or plume sources in Nb/La and Zr/Ba ratios [33]. Zr/Ba around 0.4–0.6 and Nb/La ratios between 0.45 and 0.6 for Ferrar basalts and andesites (Fig. 3) fall near the continental mantle lithosphere field [33,34]. A detectable contribution from an asthenospheric or plume source in Ferrar magmas is not evident. However, the low Nb/La signature is also typical of crustally contaminated magmas. Therefore, clear discrimination between crustal and subcontinental mantle lithosphere sources for the Ferrar basalts is not possible based on these parameters alone.

4.1. Os, Sr and O isotopic evidence

The Os isotopic ratio provides a powerful tool for distinguishing between crustal and subcontinental mantle lithosphere sources. It must, however, be demonstrated that the Re/Os systematics reflect magmatic processes, since Os may be mobile under oxidizing conditions, causing spurious and high Re/Os ratios. Os concentrations and Re/Os ratios in our Ferrar samples strongly correlate with differ-

ent parameters of both fractionation and oxidation. However, perfectly fresh rocks, as well as slightly altered and oxidized sills or vesicular flows, all fall on the same trend relating Re/Os to Mg#, suggesting that alteration does not control this correlation. Thus, the Os concentrations and Re/Os ratios were, at most, only slightly affected by secondary processes. More evidence that the Re/Os ratios were not greatly perturbed by alteration comes from $^{187}Re/^{188}Os$ correlation with $^{187}Os/^{188}Os$ (Fig. 4), giving an age of 172 ± 5 Ma and an initial $^{187}Os/^{188}Os = 0.194 \pm 0.023$. The MSWD of this isochron is 8.6 (using a program by F. Albarède, based on [35]). This age is within error of the best available Ar–Ar dates (177 ± 0.2 Ma, [21]) suggesting it is geologically meaningful.

Mantle Os isotopic compositions are slightly heterogeneous for different reservoirs [13,17,29,36–45]: The subcontinental mantle lithosphere has depleted $^{187}Os/^{188}Os$ ratios in the range 0.105–0.131, with values up to 0.138 for some lithospheric xenoliths. MORB falls in the range 0.132–0.158, with highest values for Indian Ocean MORB of 0.205, although more radiogenic values may reflect incorporation of oceanic sediment or seawater. The plume sources of OIB basalts have $^{187}Os/^{188}Os$ ratios from 0.120 to 0.150. It is unrealistic to assess different mantle sources for Ferrar magmas based on our Os data because of the large analytical error on the measured $^{187}Os/^{188}Os$ ratios caused by the very low Os concentrations (generally less than 10 ppt), and the large corrections that must be made for radiogenic growth of ^{187}Os since emplacement (over 95% of the ^{187}Os in sample BRI-29 was radiogenic). One age-corrected sample even gives a negative $^{187}Os/^{188}Os$ value, with its error reaching into the range of the other samples. However, we can still conclude that the initial Os isotope ratios (within error) fall close to mantle values for MORB, OIB and lithospheric mantle and that the Os isotope ratios are much lower than those of any typical continental crustal rocks [18]. However, the radiogenic Sr and unradiogenic Nd of our samples, well outside the range of OIBs, rule out a derivation from asthenospheric or plume mantle. The question then remains: Do these rocks represent melts of the enriched subcontinental mantle lithosphere, or melts from the convecting mantle that subsequently suffered crustal contamination?

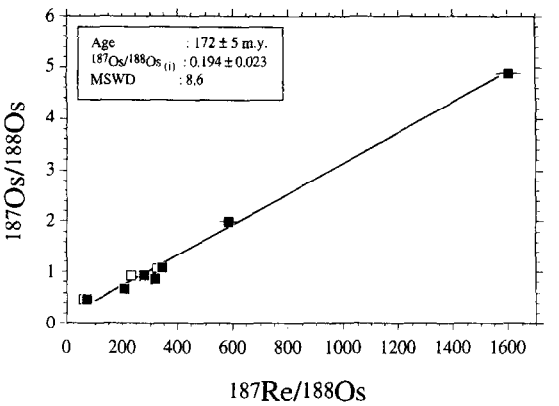

Fig. 4. Re–Os isochron assuming uncorrelated errors. ■ = powder splits with the better in-run precision used in the regression calculation, □ = duplicates. 2s-m in-run uncertainties were used for the errors on the $^{187}Os/^{188}Os$ ratios. A ±25 ppt error on $^{187}Re/^{188}Os$ ratios derives from uncertainties in the Re reproducibility and the Re blank correction. This value was used to calculate the $^{187}Re/^{188}Os$ errors used in the regression. Errors on $^{187}Re/^{188}Os$ and $^{187}Os/^{188}Os$ ratios are within the limits of the data symbols, except for $^{187}Re/^{188}Os$ for the two high $^{187}Re/^{188}Os$ samples. The MSWD (8.6) varies significantly with the choice of errors used in the regression.

Simple mixing relations between depleted peridotites (lithospheric enrichment model) and mantle magmas (assimilation model), and enriched upper and lower crustal reservoirs are tested in $^{187}Os/^{188}Os$–$^{87}Sr/^{86}Sr$ and $^{87}Sr/^{86}Sr$–$\delta^{18}O$ diagrams (Figs. 5 and 6). Sr and Os concentrations and isotopic ratios of the upper crustal end-member were chosen to be typical of terrigenous sediments [18,46]. While we have no direct knowledge of the Os isotopic composition of the continental crust underlying the Ferrar province, the high $^{87}Sr/^{86}Sr$ ratios, low $^{143}Nd/^{144}Nd$ ratios, and high $^{207}Pb/^{204}Pb$ (relative to $^{206}Pb/^{204}Pb$) ratios of the Ferrar lavas indicate that a crustal contaminant would have to be old. Metamorphic and igneous ages from the Ross Orogeny range from 480 to 560 Ma while Nd crustal residence ages range from 1.3 to 1.8 Ga [47,48]. Granitoids at Walker Rocks, near our sampling sites, gave an age of 525 ± 5 Ma (own unpublished data). Given the Nd model ages and the absence of $^{187}Os/^{188}Os$ data on crustal rocks from the Transantarctic Mountains it is conservative to assume $^{187}Os/^{188}Os$ ratios at least as high as the terrigenous sediment average ($^{187}Os/^{188}Os = 1.2$,

[18]) for potential upper crustal contaminants. This sediment average thus probably underestimates the average upper crustal ratio [18]. This suggestion is supported by river sediment leachate data [49], which imply that the soluble phases of crustal rocks may contain Os more radiogenic than that of bulk sediments. In addition to upper crustal assimilation, we will also consider contamination by lower crust, using isotopic compositions of xenoliths from Ross Sea volcanics and from the Chudleigh province in northeast Australia [50–52].

4.2. Upper crustal assimilation

We have combined all available data on crustal rocks from the Transantarctic Mountains and made a choice from this data set as to a likely isotopic and trace element composition of the middle to upper crust (Figs. 5 and 6). AFC processes are well documented for more evolved Ferrar rocks [6,7], where parameters of differentiation correlate with isotopic parameters and Sr and Nd isotopic compositions are even more, or even less, radiogenic than in the rocks considered here. The crustal end-member derived from such assimilation trends is silicic, high in Sr, low in Nd and heavy in O isotopes. We argue that assimilation of such upper crustal rocks is unlikely to explain the enriched isotopic and trace element systematics of our mafic Ferrar rocks.

Eight mixing hyperbolae have been calculated in a Sr–Os isotope diagram (Fig. 5), between crust and mantle peridotite for the lithosphere enrichment model (curves A and F) and between crust and mantle-derived picritic melt (B, G and H) and mantle basalt (C, D and E) for the assimilation model. The Os concentration of the basalt (15 ppt) is comparable to that of our most primitive sample TPS-02. This basalt has a Mg# of 71.9 (all $Fe = Fe^{2+}$) but lacks petrographic evidence of olivine accumulation. We therefore argue that this magma could have been in equilibrium with a mantle source and thus provides a possible end-member for crustal assimilation models. The picrite magma was assumed to have 1000 ppt Os and the mantle peridotite 3000 ppt. Crustal Os contents are 50 and 10 ppt for upper and lower crust, respectively.

The Sr content of the crustal end-member provides a major control on the mixing lines. Therefore Sr has been varied over reasonable ranges in crustal compositions (100 ppm and 300 ppm). Mixing curves (Fig. 5) for contamination of picrite magma (B and G) and mixing between mantle peridotite and crustal material (A, F and source contamination) fall close to our $^{187}Os/^{188}Os$ and $^{87}Sr/^{86}Sr$ data. However, the mixing proportions vary greatly. Bulk mixing between basaltic magmas and upper crust (C and D) produces curves that plot well above the data field. Upper crustal assimilation by basaltic magmas (C and D) by either bulk mixing or AFC-type processes, which will produce even higher $^{187}Os/^{188}Os$ ratios, can thus be ruled out.

Of the remaining options, bulk mixing between upper crust and picritic magma (curves B and G) are also untenable, since energy balance considerations [53] require that incorporation of large amounts of crust (40–60% for case B, and 20–35% for case G) will be accompanied by extensive fractional crystallization. Since Os is highly compatible ($D_{olivine/basalt} \sim 20$, [54]) such crystallization will rapidly decrease the magmatic Os content, rendering the Os isotopic ratio susceptible to the effects of crustal assimilation. If we assume a picrite magma with 18–20% MgO and 1000 ppt Os, about 20–25% fractionation of olivine would be needed to explain the difference in MgO and Os content between the presumed picrite and our most mafic sample (15 ppt Os). If assimilation of crust is assumed and accompanied by cooling and crystallization, then 10% fractional crystallization results in a concentration of 135 ppt Os. At this Os content, mixing curves would pass through only the two most radiogenic samples. Thus fractional crystallization would be limited to less than 10% throughout the entire assimilation process.

Among our samples, we see no relationship between initial Os isotopic ratio and degree of fractionation. In fact, the most fractionated sample, BRI-29 (Mg# = 27, [Os] = 4 ppt) has an initial $^{187}Os/^{188}Os$ ratio that is within error of that of TPS-02, the most primitive sample (Mg# = 71.9, [Os] = 15 ppt). Thus, simple AFC processes can be rejected. More complicated models involving magma replenishment are considered below.

Mixing relations in $\delta^{18}O$–$^{87}Sr/^{86}Sr$ space are shown in Fig. 6. Curve A represents mixing between a mantle peridotite and subducted sediments (enrichment model, as in Fig. 5). The field between curves

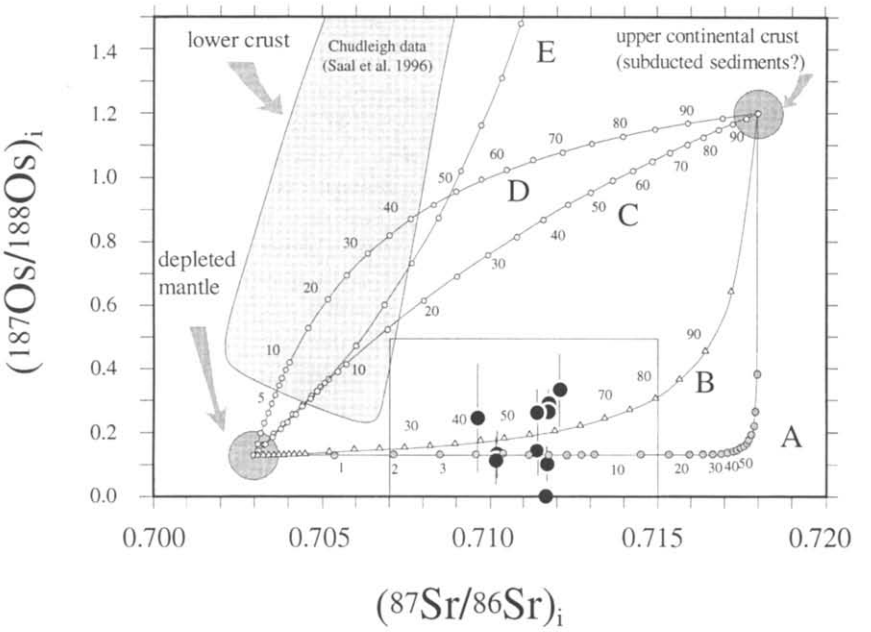

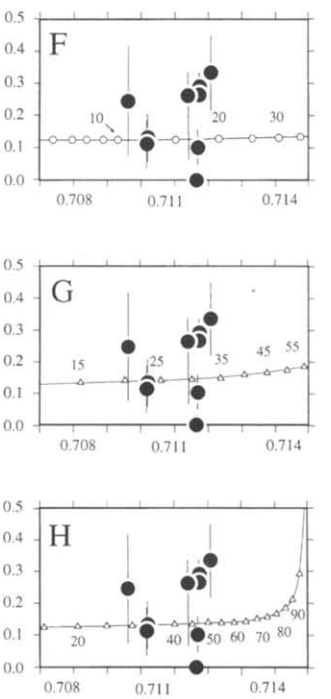

		Sr (ppm)	Os (ppt)
A	peridotite	16	3000
	crust	300	50
B	picrite	100	1000
	crust	100	50
C	basalt	150	15
	crust	300	50
D	basalt	150	15
	crust	100	50
E	basalt	150	15
	lower crust	300	10
F	peridotite	16	3000
	crust	100	50
G	picrite	100	1000
	crust	300	50
H	picrite	100	1000
	lower crust	300	10

peridotite, picrite, basalt:

$^{187}Os/^{188}Os = 0.1276$

$^{87}Sr/^{86}Sr = 0.7030$

Crust	(A-D, F, G):	(E, H):
$^{187}Os/^{188}Os$ =	1.2035	3.5
$^{87}Sr/^{86}Sr$ =	0.7180	0.715

Fig. 5. Initial $^{187}Os/^{188}Os$ vs. initial $^{87}Sr/^{86}Sr$. Model curves represent mixing between mantle peridotite and crustal sediments (source contamination) and mantle magmas (basalts and picrites) and crust (crustal contamination). The crustal end-member was chosen to be variable in Sr content (100–300 ppm). The $^{187}Os/^{188}Os$–$^{87}Sr/^{86}Sr$ reference data field for lower crustal xenoliths from the Chudleigh province in NE Australia was kindly made available by Alberto Saal ([51] and Saal et al. unpubl. data).

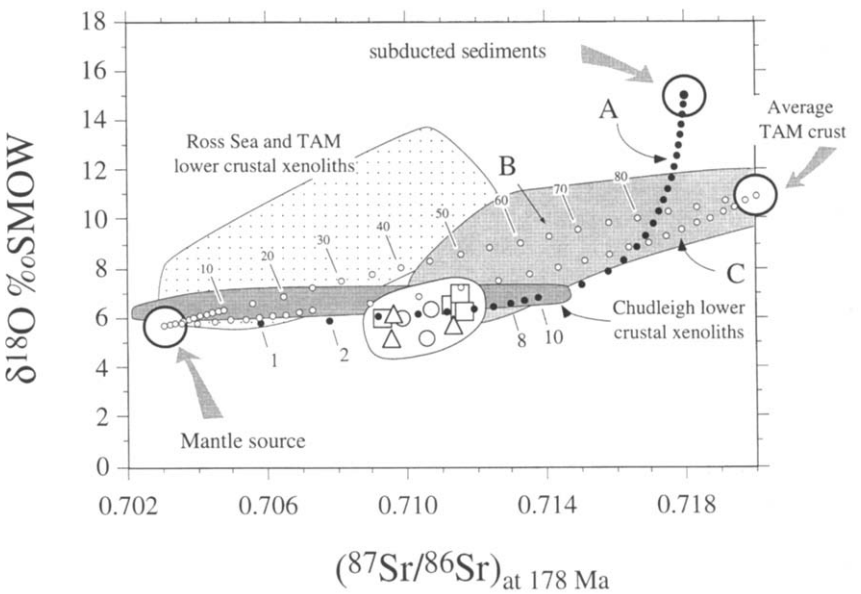

Fig. 6. Initial $^{87}Sr/^{86}Sr$ vs. $\delta^{18}O$ mixing curves and Ferrar whole rock and mineral data. (A) Source contamination: peridotite (Sr = 16 ppm, $^{87}Sr/^{86}Sr = 0.703$) contaminated by sediments (Sr = 300 ppm, $^{87}Sr/^{86}Sr = 0.718$). (B) Crustal contamination of picrite (Sr = 100 ppm, $^{87}Sr/^{86}Sr = 0.703$) with Sr-poor crust (Sr = 100 ppm, $^{87}Sr/^{86}Sr = 0.720$). (C) crustal contamination of picrite (Sr = 100 ppm, $^{87}Sr/^{86}Sr = 0.703$) with Sr-rich crust (Sr = 300 ppm, $^{87}Sr/^{86}Sr = 0.720$). O concentration: 48% for sediment or crust and 40% for mantle peridotite and melts. The crustal sediment end-member has $\delta^{18}O = 15‰$ and mantle values are $\delta^{18}O = 5.70‰$ SMOW. The plotted data from our Ferrar rocks were screened for alteration and represent fresh whole rocks (□); separated clean clinopyroxenes (△); and plagioclase (○). The data field for Chudleigh lower crustal xenoliths is from [56], data for xenoliths from the Ross Sea and TAM region are from [50]. Granitoids of the Ross Orogeny are of transitional S- and I-type, representing the composition of the TAM crust. All Sr isotopic ratios have been calculated as initials at 178 Ma, the age of Ferrar magmatism.

B and C covers mixing relations (assimilation model) between basaltic and picritic melts and various crustal compositions (Sr = 100–300 ppm) which have been approximated from our own and published data on crustal rocks from the TAM [48]. Curves for mixing between sediments and basaltic and picritic magmas are highly concave (not shown) and plot well above the data field. Our data from fresh Ferrar rocks and clean mineral separates fall on the peridotite–sediment mixing line (A). Only the high-Sr (300 ppm) TAM crust–picrite mixing trend (curve C, Fig. 6) falls close to the upper $\delta^{18}O$ range of the Ferrar field. Mixing relations would suggest 15–25% crust. A basalt–Sr-rich crust mix (not shown) would fall between the two curves B and C and above the Ferrar data.

4.3. Lower crustal assimilation

Another possible crustal assimilant is lower continental crust, which can be rather unradiogenic in Sr and low in $\delta^{18}O$. Such lower crust has been documented from xenoliths, for example, those found in the Tertiary to Recent volcanics from the Ross Sea and Transantarctic Mountain region ([50], and own unpublished data) and Chudleigh and McBride volcanic provinces (northeast Australia, [51,52,55]). While the TAM and Ross Sea lower crustal xenoliths may directly relate to assimilation by Ferrar magmas, the Chudleigh xenolith suite from northeast Australia cannot be correlated directly with the lower crust below the TAM. However, the Chudleigh xenoliths have now been analysed also for $^{187}Os/^{188}Os$ ([51], and Saal et al., 1996, in prep.) and the hypothesis of lower crustal assimilation can now be tested for Os isotopes as well (Figs. 5 and 6).

The majority of the Sr–Os–O and Sr–O data for the Chudleigh and Ross Sea/TAM xenoliths, respectively, fall entirely outside any meaningful end-member composition for a lower crustal bulk mixing trend for Ferrar magmas. Binary mixing between the most radiogenic and extreme Chudleigh range and

basalt from a depleted mantle source produces mixing curves (Fig. 5E) that plot well above the Ferrar data, even if very low Os (10 ppt) and high Sr concentrations (300 ppm) are assumed for the contaminant. Basalt bulk assimilation of lower crust can thus be ruled out. However, mixtures between this extreme end-member and picritic magmas pass through the data field (Fig. 5, curve H), but only at crustal proportions of 30–50%. Such large amounts of crust are unlikely for magmas that range from mafic (Mg# = 71.9) to intermediate compositions, while AFC processes, without magma replenishment, will lead to much more radiogenic Os compositions. Thus, both bulk mixing and AFC lower crustal contamination of picritic magmas can be excluded.

A further argument against the picrite contamination model comes from consideration of the coupled O and Sr isotope data (Fig. 6). It is obvious that assimilation with lower crust comparable to the TAM and Ross Sea xenoliths cannot explain the enriched signature of Ferrar lavas. High $^{87}Sr/^{86}Sr$ is correlated with high $\delta^{18}O$ for the lower crust in the Ross Sea and TAM, and the majority of the data fall to the low $^{87}Sr/^{86}Sr$ side of the Ferrar data field. Thus, even though low $\delta^{18}O$ rocks do exist at the base of the TAM and Ross Sea crust, their typical $^{87}Sr/^{86}Sr$ ratios are much too low for them to be potential assimilants. This is also true for the majority of the Chudleigh data [51]. Only the most enriched Chudleigh compositions can serve as a mixing end-member. We conclude that the Sr–Os–O systematics of known lower crust are incapable of explaining the enriched signature of Ferrar magmas through bulk mixing or AFC processes.

4.4. AFC models with magma replenishment

Several models for flood basalt genesis [8,57,58] combine AFC processes with magma chamber refilling, fractionation, and tapping processes. Taking equation 10 from [58] and a typical $^{87}Sr/^{86}Sr$ ratio of 0.711 for the observed magmas, we calculated the $^{187}Os/^{188}Os$ and $\delta^{18}O$ ratios that would result from

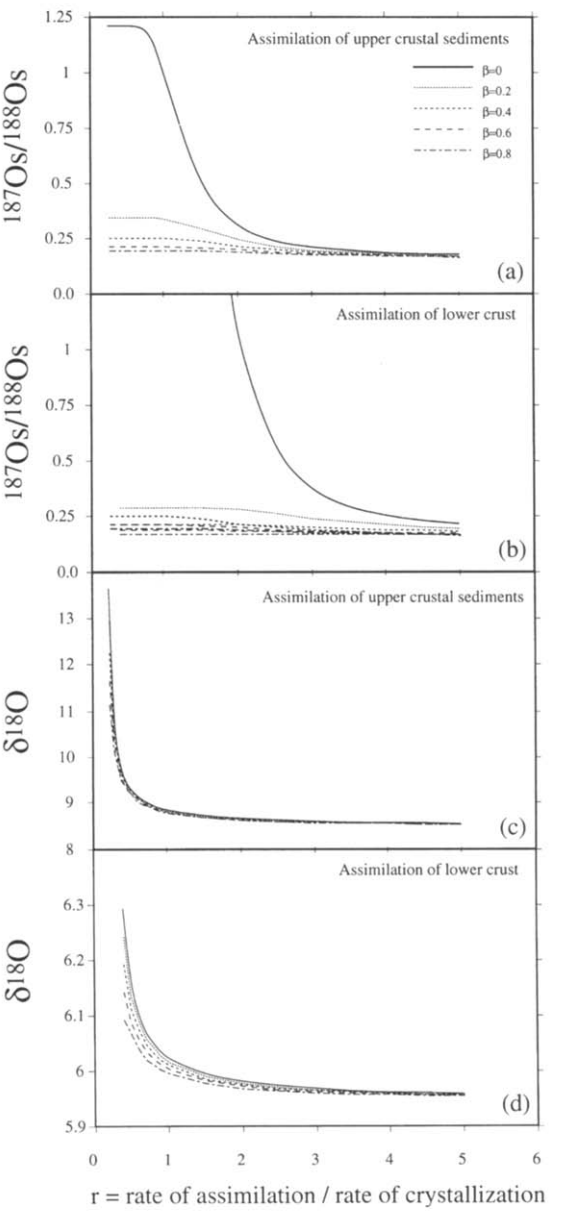

Fig. 7. $^{187}Os/^{188}Os$ and $\delta^{18}O$ values obtained for replenishment-AFC model calculations [58], as a function of r (rate of crustal assimilation/rate of fractional crystallization) and β (rate of magma replenishment/rate of assimilation), using a $^{87}Sr/^{86}Sr$ ratio for the contaminated magma of 0.711. The following values were used: $D_{Sr} = 0.1$; $D_{Os} = 20$; $D_O = 1$. Concentrations and isotopic ratios for original and recharge magmas were: Sr = 100 ppm, $^{87}Sr/^{86}Sr = 0.703$; Os = 1000 ppt, $^{187}Os/^{188}Os = 0.1276$; O = 40%, $\delta^{18}O = 5.5$. Values for the crustal assimilant were: (a) and (c) Upper crustal sediments: Sr = 300 ppm, $^{87}Sr/^{86}Sr = 0.718$; Os = 50 ppt, $^{187}Os/^{188}Os = 1.2035$; O = 48%, $\delta^{18}O = 15$. (b) and (d) Lower crust: Sr = 300 ppm, $^{87}Sr/^{86}Sr = 0.715$; Os = 10 ppt, and the extreme $^{187}Os/^{188}Os = 3.5$ of the Chudleigh data [51]; O = 48%, $\delta^{18}O = 6.5$.

assuming various rates of r (rate of assimilation of crust/rate of fractional crystallization) and β (rate of magma replenishment/rate of assimilation) for a picritic magma undergoing this process. Results for upper crustal and lower crustal contamination are plotted in Fig. 7. Parameters used in the calculations are listed in the caption. Note that as r becomes very large, the case of simple binary mixing is approached. The case of $\beta = 0$ is equivalent to pure AFC. For both upper and lower crustal contamination (Fig. 7a,b), AFC leads to $^{187}Os/^{188}Os$ ratios much greater than those observed, except at unrealistically high values of r, which should have an upper limit of about 1. However, at higher rates of magma replenishment ($\beta > 0.6$) assimilation of both upper and lower crustal material can produce the observed Os isotopic ratios. This is true, however, only for picritic magmas that start with high Os concentrations.

Oxygen isotopes provide a better constraint. For the case of upper crustal assimilation, assuming a $\delta^{18}O$ value of 15, typical of average sediments for the contaminant, $\delta^{18}O$ never approaches the observed values of about 6, regardless of the values chosen for r and β (Fig. 7c). Contamination by average TAM granitic crust (not shown), with $\delta^{18}O$ equal to about 11, works better, but still produces $\delta^{18}O$ values (~ 7) that only skim the top of the data field. For lower crustal assimilation, the observed oxygen compositions can be produced, assuming a contaminant composition comparable to those of the Chudleigh xenoliths with the most radiogenic Sr ratios (Fig. 7d). However, it should be noted that the great majority of the lower crustal xenoliths from the Ross Sea, TAM and Chudleigh regions do not provide suitable assimilants.

A serious problem with the replenishment-AFC model is that it tends to produce high incompatible element contents, while the Ferrar lavas and equivalent Tasmanian dolerites have surprisingly low concentrations of these elements [10,59,60]. This is perhaps not a fatal flaw in the model, since the end-member compositions are only poorly known. However, it does pose some constraints on these compositions. In particular, it leads to the conclusion that the Sr concentration of the assimilant must be fairly high. Otherwise, very large amounts of assimilation would be needed to reach the observed $^{87}Sr/^{86}Sr$ ratios, which would be coupled with large amounts of fractional crystallization, driving up the incompatible element contents in the magma to unrealistically high levels.

To sum up, replenishment-AFC models could explain the observed Sr, Os and O isotopic data. However, for this to be true, the following conditions must be met: The initial magma must have high Os concentrations, and the rate of replenishment relative to the rate of assimilation must be moderate to high. The assimilant must have high $^{87}Sr/^{86}Sr$ ratios coupled with low $\delta^{18}O$ values and high Sr contents, which rules out the majority of lower crustal xenoliths found in the Antarctic region, as well as typical upper crustal compositions, including sediments. Finally, such lower crust must also impart a trace element pattern of terrestrial sediments onto the contaminated magmas.

Considering these requirements, the observed range of lower crustal compositions, and the absence of direct evidence for derivation of Ferrar flood basalts from picrite parents, our preferred interpretation is that assimilation is not responsible for the enriched characteristics of the Ferrar magmas. In contrast, peridotite–sediment mixing and melting of such enriched lithosphere could explain the observed geochemical characteristics. We will therefore test enrichment and melting of a lithospheric mantle source as an alternative model.

4.5. Trace element melting models

Ferrar rocks are characterized by trace element patterns that parallel those of terrestrial shales ([59,60], Fig. 2). A sedimentary origin for the contaminant is also suggested by their high $^{207}Pb/^{204}Pb$ relative to $^{206}Pb/^{204}Pb$ ratios. Thus it is reasonable to model the enriched signature of Ferrar magmas by melting a depleted mantle source that has been enriched in the mantle lithosphere by introduction of a sediment component during subduction [9,10]. We performed batch melting calculations on a source assumed to consist of a mixture of depleted MORB source mantle and sediment (Fig. 8) with sediment proportions varying between 1% and 10% and batch melting between 1% and 30%. We find the best agreement between observed (TPS-02, Mg# = 71.9) and calculated compositions for 3% sediment in the

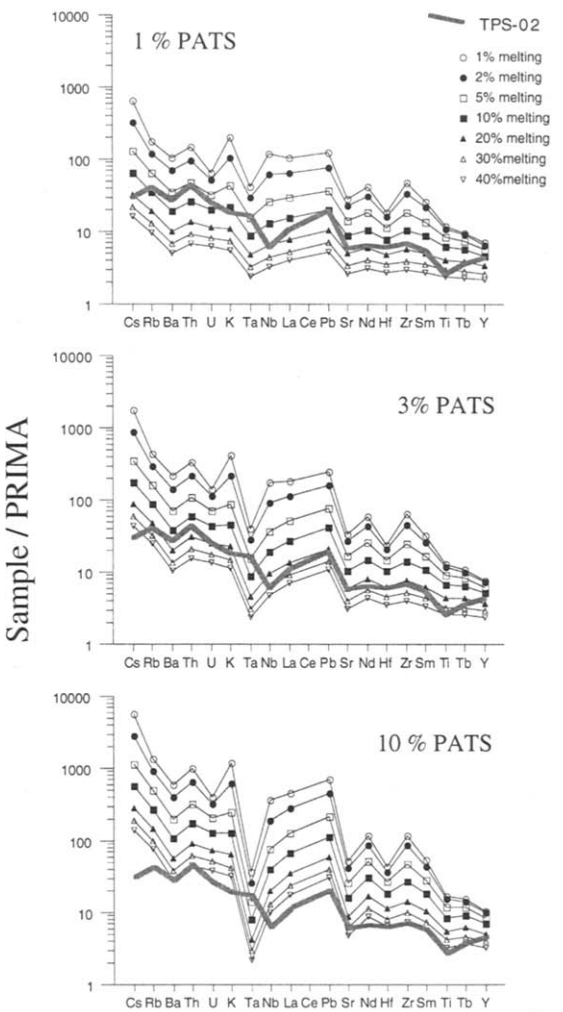

Fig. 8. Trace element melting models of sediment–peridotite mixtures. Pre-contamination peridotite compositions are based on a depleted MORB source composition [61], while sediment compositions are based on the post-Archean terrestrial shale average [46]. A batch melting process (1–40%) is assumed. The best fit between the model and the measured trace element data on Ferrar rocks is found at 15–20% melting of a source enriched by contamination with 3% sediment.

source (consistent with the peridotite–sediment mixing curves) and 15–20% melting. Deviations between the model and observation could be due in part to the fact that incorporation of sediment into the mantle by subduction will undoubtedly result in trace element fractionation. Assuming bulk addition of a sediment composition, therefore, is the simplest possible model.

We note that the melting degree is rather high but is in agreement with the low overall incompatible trace element contents. Furthermore, addition of presumably water-rich sediments would facilitate melt production. In fact, if melting of hydrous peridotite is permitted, then large amounts of melt may be obtained from a lithospheric mantle [64]. The model of melting sediment-enriched lithosphere is capable of explaining both the isotope characteristics and the trace element patterns of Ferrar magmas. It is also more capable of explaining the surprising spatial uniformity of these characteristics, which may vary little over several thousand kilometres [10], since marine [62] and terrestrial sediments [18,63] display less isotopic diversity than Antarctic crustal rocks. Thus the homogeneity, as well as the isotopic and trace element compositions of these lavas, can be explained by the sediment enrichment model.

5. Conclusions

Major and trace element data, as well as Sr, Nd, and Pb isotope compositions, from mafic to intermediate lavas and sills from the Ferrar flood basalt province (Prince Albert Mountains) suggest a contribution of a strongly enriched component. Even our most mafic sample (Mg# = 71.9) has crustal Sr and Nd isotope compositions, and a trace element pattern similar to those of terrestrial sediments, but falls into the mantle range with respect to its O and Os isotopes.

The combination of the $^{187}Os/^{188}Os$–$^{87}Sr/^{86}Sr$ and $\delta^{18}O$–$^{87}Sr/^{86}Sr$ systematics allows us to exclude both upper and lower crustal assimilation by basaltic magmas. AFC processes, coupled with replenishment of picritic magma, could explain the Os isotopic data; however, only by assuming a crustal component with low $\delta^{18}O$ and high $^{87}Sr/^{86}Sr$ isotope compositions and high Sr contents (> 300 ppm), which excludes typical upper crustal sediments. The appropriate Sr and O isotopic compositions also do not exist among lower crustal xenoliths from the TAM and Ross Sea areas. The required compositions, except for high Sr contents, are found only among extreme members of the Chudleigh lower crustal xenolith suite of northeast Australia. Assimilation models can thus not readily explain the low

incompatible element contents and the trace element patterns of Ferrar rocks that mimic those of terrestrial sediments.

Our data can be reconciled by mixing mantle peridotite and crustal material (Fig. 5 curves A and E), suggesting a subcontinental mantle lithosphere enriched in crustal material as a source for Ferrar magmas. Melting models show that about 15–20% melting of a peridotite enriched by about 3% sedimentary material reproduces the trace element pattern observed in mafic Ferrar lavas. Similar amounts of source contamination have been invoked previously [10,59,60]. A mechanism for enriching the lithosphere may have been provided by the subduction zone that existed on the Pacific margin of Gondwana until the Jurassic.

The Nb/La–Zr/Ba relations exclude a detectable plume component. Constant Nb/La with variable Zr/Ba, if caused by sediment contamination of a mantle source, would have to result from a sediment composition highly variable in Ba, which is a reasonable assumption considering the large range of Ba values found for pelagic sediments.

A plume component in the Ferrar source can thus not be distinguished in either the trace element or the isotope data. It is possible that such a component exists but is masked by the lithospheric signal. However, the extent of a plume contribution is limited by the fact that it would have to be counter-balanced by even more extreme incompatible element enrichment of the lithosphere.

Melting of a hydrous mantle lithosphere may have been induced by a thermal contribution from a plume.

Irrespective of the potential role of a presumed Ferrar plume, crustal contamination of the magmas during their evolution to explain the enriched Sr and Pb isotopes, unradiogenic Nd isotopes and crustal trace element patterns appears to be less likely than direct melting of an enriched mantle lithosphere.

Acknowledgements

The Bundesanstalt für Geowissenschaften und Rohstoffe invited us to the GANOVEX VI and VII expeditions, field equipment was made available by the Alfred Wegener Institut für Polar- und Meeresforschung. This study was funded by the DFG-Project "Ferrar-Laven" (Wö 362/7-1,2). Financial support for the stay of MM in Nancy was provided by the DAAD (512 006 594 4). Al Hofmann supported this study in many ways and provided facilities for Sr, Nd, and Pb isotope measurements at the Max Planck Institut in Mainz. Klaus Mezger helped with the Pb isotope analyses. We thank Nick Arndt and Steve Shirey for critical comments which focused our arguments. Last, but certainly not least, we are indebted to Alberto Saal from Woods Hole and his co-workers for providing and letting us use his unpublished Os isotope data on Chudleigh xenoliths. Without his help it would have been difficult to assess lower crustal assimilation models. *[CL]*

References

[1] R. White and D. McKenzie, Magmatism at rift zones: the generation of volcanic continental margins and flood basalts, J. Geophys. Res. 94, 7685–7729, 1989.

[2] I.H. Campbell and R.W. Griffiths, Implications of mantle plume structure for the evolution of flood basalts, Earth Planet. Sci. Lett. 99, 79–93, 1990.

[3] D.L. Anderson, Superplumes or supercontinents?, Geology 22, 39–42, 1994.

[4] F. Coffin-Millard and O. Eldholm, Volcanism and continental break-up; a global compilation of large igneous provinces, in: Magmatism and the Causes of Continental Break-up, B.C. Storey, T. Alabaster and R.J. Pankhurst, eds., Geol. Soc. London Spec. Publ. 68, 17–30, 1992.

[5] G. Faure, J.R. Bowman, D.H. Elliot and D.M. Jones, The initial $^{87}Sr/^{86}Sr$ ratios of the Kirwan Volcanics of Dronning Maud land: Comparison with the Kirkpatrick Basalt, Transantarctic Mountains, Contrib. Mineral. Petrol. 48, 153–169, 1974.

[6] J. Hoefs, G. Faure and D.H. Elliot, Correlation of $\delta^{18}O$ and initial $^{87}Sr/^{86}Sr$ ratios in Kirkpatrick Basalt at Mt. Falla, Transantarctic Mountains, Contrib. Mineral. Petrol. 75, 199–203, 1980.

[7] T.M. Mensing, G. Faure, L.M. Jones, J.R. Bowman and J. Hoefs, Petrogenesis of the Kirkpatrick Basalt, Solo Nunatak, Northern Victoria Land, Antarctica, based on isotopic compositions of strontium, oxygen and sulfur, Contrib. Mineral. Petrol. 87, 101–108, 1984.

[8] Z.X. Peng, L.L. Mahoney, P. Hopper, C. Harris and J. Beane, A role for lower continental crust in flood basalt genesis? Isotopic and incompatible element study of the lower six formations of the western Deccan Traps, Geochim. Cosmochim. Acta 58, 267–288, 1994.

[9] D.H. Elliot, Jurassic magmatism and tectonism associated with Gondwanaland break-up: an Antarctic perspective, in: Magmatism and the Causes of Continental Break-up, B.C.

Storey, T. Alabaster and R.J. Pankhurst, eds., Geol. Soc. London Spec. Publ. 68, 165–184, 1992.

[10] J.M. Hergt, B.W. Chappel, G. Faure and T.M. Mensing, The geochemistry of Jurassic dolerites from Portal Peak, Antarctica, Contrib. Mineral. Petrol. 102, 298–305, 1989.

[11] T.S. Brewer, J.M. Hergt, C.J. Hawkesworth, D. Rex and B.C. Storey, Coats Land dolerites and the generation of Antarctic continental flood basalts, in: Magmatism and the Causes of Continental Break-up, B. Storey, T. Alabaster and R. Pankhurst, eds., Geol. Soc. London Spec. Publ. 68, 185–208, 1992.

[12] D. Peate and C.J. Hawkesworth, Lithospheric to asthenospheric transition in low-Ti flood basalts from southern Paraná, Brazil, Chem. Geol. 127, 1–24, 1996.

[13] E.H. Hauri and S.R. Hart, Re–Os isotope systematics of HIMU and EMII oceanic island basalts from the south Pacific Ocean, Earth Planet. Sci. Lett. 114, 353–371, 1993.

[14] C.J. Allègre and J.-M. Luck, Osmium isotopes as petrogenetic and geological tracers, Earth Planet. Sci. Lett. 48, 148–154, 1980.

[15] C.E. Martin, Osmium isotopic characteristics of mantle derived rocks, Geochim. Cosmochim. Acta 55, 1421–1434, 1991.

[16] W.J. Pegram and C.J. Allègre, Osmium isotopic compositions from oceanic basalts, Earth Planet. Sci. Lett. 111, 59–68, 1992.

[17] L. Reisberg, A. Zindler, F. Manrcantonio, W. White, D. Wyman and B. Weaver, Os isotope systematics in ocean island basalts, Earth Planet. Sci. Lett. 120, 149–167, 1993.

[18] B.K. Esser and K.K. Turekian, The osmium isotopic composition of the continental crust, Geochim. Cosmochim. Acta 57, 3093–3104, 1993.

[19] R.M. Ellam, R.W. Carlson and S.B. Shirey, Evidence from Re–Os isotopes for plume–lithosphere mixing in Karoo flood basalt genesis, Nature 359, 718–721, 1992.

[20] M.R. Horan, R.J. Walker, V.A. Fedorenko and G.K. Czamanske, Geochim. Cosmochim. Acta 59, 5159–5168, 1995.

[21] A. Heimann, T.H. Fleming, D.H. Elliot and K.A. Foland, A short interval of Jurassic continental flood basalt volcanism in Antarctica as demonstrated by $^{40}Ar/^{39}Ar$ geochronology, Earth Planet. Sci. Lett. 121, 19–41, 1994.

[22] D.H. Elliot, Jurassic magmatism and tectonism associated with Gondwanaland break-up: an Antarctic perspective, in: Magmatism and the Causes of Continental break-up, B.C. Storey, T. Alabaster and R.J. Pankhurst, eds., Geol. Soc. London Spec. Publ. 68, 165–184, 1992.

[23] P.R. Kyle, D. Elliot and J. Sutter, Jurassic Ferrar Supergroup tholeiites from the Transantarctic Mountains, Antarctica, and their relationship to the initial fragmentation of Gondwana, in: Gondwana Five, M. Cresswell and P. Vella, eds., pp. 283–287, Balkema, Rotterdam, 1981.

[24] G. Kleinschmidt and F. Tessensohn, Early Paleozoic westward directed subduction at the Pacific margin of Antarctica; in: Gondwana Six: Structures, Tectonics and Geophysics, G.D. McKenzie, ed., AGU 40, 89–105, 1987.

[25] F. Tessensohn, K. Duphorn, H. Jordan, G. Kleinschmidt, D.N.B. Skinner, U. Vetter, T.O. Wright and D. Wyborn, Geological comparison of basement units in north Victoria Land, Antarctica, Geol. Jahrb. B41, 31–88, 1981.

[26] J.W. Collinson, The paleo-Pacific margin as seen from East Antarctica, in: Geological Evolution of Antarctica, M.R.A. Thomson, J.W. Crame and J.W. Thomson, eds., pp. 199–204, Cambridge Univ. Press, 1991.

[27] T.H. Fleming, K.A. Foland and D.H. Elliot, Direct dating of mid-Cretaceous alteration of the Kirkpatrick Basalt in North Victoria Land: Argon-40/Argon-39 and Rubidium/Strontium ages of Apophyllite, Antarctic J. US, 1993.

[28] C. Harris, J.S. Marsh, A.R. Duncan and A. Erlank, The petrogenesis of the Kirwan Basalts of Dronning Maud Land, Antarctica, J. Petrol. 31, 341–369, 1990.

[29] R.J. Walker, R.W. Carlson, S.B. Shirey and F.R. Boyd, Os, Sr, Nd and Pb isotope systematics of southern African peridotite xenoliths: implications for the chemical evolution of subcontinental mantle, Geochim. Cosmochim. Acta 53, 1583–1595, 1989.

[30] J. Volkening, T. Walczyk and K.G. Heumann, Osmium isotope determinations by negative thermal ionization mass spectrometry, Int. J. Mass. Spectrom. Ion Phys. 105, 147–159, 1991.

[31] R.A. Creaser, D. Papanastassiou and G.J. Wasserburg, Negative thermal ion mass spectrometry of osmium, rhenium, and iridium, Geochim. Cosmochim. Acta 55, 397–401, 1991.

[32] A.W. Hofmann, Chemical differentiation of the Earth: the relationship between mantle, continental crust, and oceanic crust, Earth Planet. Sci. Lett. 90, 297–314, 1988.

[33] C.J. Hawkesworth and K. Gallagher, Mantle hotspots, plumes and regional tectonics as causes of intraplate magmatism, Terra Nova 5, 552–559, 1993.

[34] N.T. Arndt and U. Christensen, The role of lithospheric mantle in continental flood volcanism: thermal and geochemical constraints, J. Geophys. Res. 97, B7, 10,967–10,981, 1992.

[35] D. York, Least squares fitting of a straight line with correlated errors, Earth Planet. Sci. Lett. 5, 320–334, 1969.

[36] J.-M. Luck and C.-J. Allègre, Osmium isotopes in ophiolites, Earth Planet. Sci. Lett. 107, 406–415, 1991.

[37] C.E. Martin, Osmium isotopic characteristics of mantle-derived rocks, Geochim. Cosmochim. Acta 55, 1421–1434, 1991.

[38] L Reisberg, C.J. Allègre and J.M. Luck, The Re–Os systematics of the Ronda ultramafic complex of southern Spain, Earth Planet. Sci. Lett. 105, 196–213, 1991.

[39] M. Roy-Barman and C.J. Allègre, $^{187}Os/^{186}Os$ in oceanic island basalts: tracing oceanic crust recyling in the mantle, Earth Planet. Sci. Lett. 129, 145–161, 1995.

[40] R.W. Carlson and A.T. Irving, Depletion and enrichment history of subcontinental lithospheric mantle: An Os, Sr, Nd, and Pb isotopic study of ultramafic xenoliths from the northwestern Wyoming craton, Earth Planet. Sci. Lett. 126, 457–472, 1994.

[41] D.G. Pearson, R.W. Carlson, S.B. Shirey, F.R. Boyd and

P.H. Nixon, Stabilisation of Archean lithospheric mantle: A Re–Os isotope study of peridotite xenoliths from the Kaapvaal craton, Earth Planet. Sci. Lett. 134, 341–357, 1995.

[42] D.G. Pearson, S.B. Shirey, R.W. Carlson, F.R. Boyd, N.P. Pokhilenko and N. Shimizu, Re–Os, Sm–Nd, and Rb–Sr isotopic evidence for thick Archean lithospheric mantle beneath the Siberian Craton modified by multistage metasomatism, Geochim. Cosmochim. Acta 59, 959–977, 1995.

[43] O.M. Burnham and N.W. Rogers, Re and Os in peridotite massifs: Implications for models of continental lithospheric mantle evolution, J. Conf. Abstr. 1, 91, 1996.

[44] D.R. Hassler and N. Shimizu, The Osmium isotopic composition of peridotitic xenoliths from the northeastern Kerguelen Islands, J. Conf. Abstr. 1, 237, 1996.

[45] P. Schiano, J.-L. Birck and C.J. Allègre, Re–Os isotope systematics of Mid-Ocenan Ridge Basalt glasses, J. Conf. Abstr. 1, 539, 1996.

[46] S. Taylor and S. McLennan, The Continental Crust: its Composition and Evolution, Blackwell, 1985.

[47] S.G. Borg and D.J. DePaolo, A tectonic model of the Antarctic Gondwana margin with implications for south-eastern Australia: isotopic and geochemical evidence, Tectonophysics 169, 339–358, 1991.

[48] S.G. Borg, D.J. DePaolo and B.M Smith, Isotopic structure and tectonics of the Central Transantarctic Mountains, J. Geophys. Res. 95, B5, 6647–6667, 1990.

[49] W.J. Pegram, B.K. Esser, S. Krishnaswami and K.K Turekian, The isotopic composition of leachable osmium from river sediments, Earth Planet. Sci. Lett. 128, 591–599, 1994.

[50] R.I. Kalamarides and J.H. Berg, Geochemistry and tectonic implications of lower-crustal granulites included in Cenozoic volcanic rocks of southern Victoria Land, in: Geological evolution of Antarctica, M.R. Thomson, A. Crame, J. Alistair, and J.W. Thomson, eds., pp. 305–310, Proc. Int. Symp. Antarct. Earth Sci., 5, Cambridge, 1991.

[51] A.E. Saal, R.L. Rudnick, G.E. Ravizza and S.R. Hart, Os isotopic composition of lower crustal xenoliths from Northern Queensland, Australia, J. Conf. Abstr. 1, 528, 1996.

[52] R.L. Rudnick, Nd and Sr isotopic compositions of lower-crustal xenoliths from north Queensland, Australia: Implications fro Nd model ages and crustal growth processes, Chem. Geol. 83, 195–208, 1996.

[53] H.P. Taylor, The effects of assimilation of country rocks by magmas on $^{18}O/^{16}O$ and $^{87}Sr/^{86}Sr$ systematics in igneous rocks, Earth Planet. Sci. Lett., 243–254, 1980.

[54] S.R. Hart and G.E. Ravizza, Os partitioning between phases in lherzolite and basalt, in: Earth Processes: Reading the Isotopic Code, A. Basu and S.R. Hart, eds., Geophys. Monogr. 95, 123–134, 1996.

[55] M.B. Fowler and R.S. Harmon, The oxygen isotope composition of lower crustal granulite xenoliths, in: Granulites and Crustal Evolution, D. Vielzeuf and Ph. Vidal, eds., pp. 493–506, Kluwer, Dordrecht, 1990.

[56] P.D. Kempton and R.S. Harmon, Oxygen isotope evidence for large-scale hybridization of the lower crust during magmatic underplating, Geochim. Cosmochim Acta 56, 971–986, 1992.

[57] K.G. Cox, A model for flood basalt genesis, J. Petrol. 21, 629–650, 1980.

[58] S.J. Aitcheson and A.H. Forrest, Quantification of crustal contamination in open magmatic systems, J. Petrol. 35, 461–488, 1994.

[59] J.M. Hergt, B.W. Cappel, M.T. McCulloch, J. MacDougall and A.R. Chivas, Geochemical and isotopic contraints on the origin of the Jurassic dolerites of Tasmania, J. Petrol. 30, 841– 883, 1989.

[60] J.M. Hergt, D.W. Peate and C.J. Hawkesworth, The petrogenesis of Mesozoic Gondwana low-Ti flood basalts, Earth Planet. Sci. Lett. 105, 134–148, 1991.

[61] D. Wood, A variably veined suboceanic upper mantle — Genetic significance for mid-ocean ridge basalts from geochemical evidence, Geology 7, 499–503, 1979.

[62] D. Ben-Othman-Dalila, W.M. White and J. Patchett, The geochemistry of marine sediments, island arc magma genesis, and crust–mantle recycling, Earth Planet. Sci. Lett. 94, 1–21, 1989.

[63] S.L. Goldstein, Decoupled evolution of Nd and Sr isotopes in the continental crust and the mantle, Nature 336, 733–738, 1988.

[64] K. Gallagher and C. Hawkesworth, Dehydration melting and the generation of continental flood basalts, Nature 358, 57–59, 1992.